Table I. Temperature Dependence of K_{disp}'[a]

$Rh_2(dimen)_2(dppm)_2^{3+}$		$Rh_2(dimen)_3(dppm)^{3+}$		$Rh_2(dimen)_4^{3+}$	
T, °C	$10^{10}K_{disp}'$[b]	T, °C	K_{disp}'[c]	T, °C	$10^{-3}K_{disp}'$[d]
20	8.3 (5)	25	1.04 (18)	25	4.5 (9)
15	5.3 (5)	4	0.94 (40)	10	4.0 (6)
5	2.3 (5)	-10	0.74 (21)	0	3.5 (7)
-1	1.3 (5)	-35	0.71 (22)	-15	2.6 (5)
-3	1.0 (5)	-50	0.53 (33)	-25	2.4 (6)

[a] Standard deviations in the last significant digit are listed in parentheses. [b] K_{disp}' is calculated from the temperature dependence of ($E^{\circ\prime}_{3+/2+}$ - $E^{\circ\prime}_{4+/3+}$) and eq 6. [c] K_{disp}' is determined by UV-vis spectroelectrochemical measurements. [d] K_{disp}' is determined by IR spectroelectrochemical measurements.

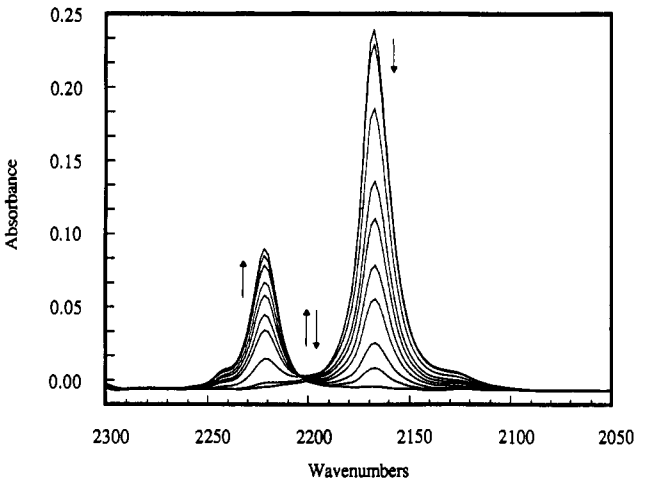

Figure 4. Plot of the IR spectral changes observed during the spectroelectrochemical oxidation of $Rh_2(dimen)_4^{2+}$ in 0.1 M $TBA^+ClO_4^-/CH_2Cl_2$. Note the lack of a distinct isosbestic point at 2200 cm^{-1} where the $Rh_2(dimen)_4^{3+}$ radical absorbs.

IR spectra of the d^7-d^7 species agree well with the spectra of other two-electron oxidized compounds of similar structure.[19]

Figure 3 shows the UV-vis spectroelectrochemical oxidation of $Rh_2(dimen)_3(dppm)^{2+}$; the analogous IR experiment is shown for $Rh_2(dimen)_4^{2+}$ in Figure 4.[20] In each case, the initial spectrum in the series corresponds to the d^8-d^8 starting material, while the final spectrum is attributed to the d^7-d^7 $2e^-$ oxidation product. Note, however, the appearance of transient absorbances (at 430 nm in the UV-vis experiment for $Rh_2(dimen)_3(dppm)^{2+}$ and 2200 cm^{-1} in the IR experiment for $Rh_2(dimen)_4^{2+}$), which increase, reach a maximum value midway through the electrolysis, and eventually disappear. By analogy to the UV-vis and IR spectra of $Rh_2(dimen)_2(dppm)_2^{3+}$ and other d^7-d^8 radicals,[21] these absorbances are assigned to $Rh_2(dimen)_3(dppm)^{3+}$ and $Rh_2(dimen)_4^{3+}$.[22] Plots of the relative concentrations of the d^8-d^8, d^7-d^8, and d^7-d^7 species as a function of the number of electrons removed allow the calculation of radical disproportionation constants at 25 °C of 1.04 (18) for $Rh_2(dimen)_3(dppm)^{3+}$ and 4.5 (9) × 10^3 for $Rh_2(dimen)_4^{3+}$; direct electrochemical data at 20 °C (eq 6) yields a value of 8.3 (5) × 10^{-10} for the disproportionation of $Rh_2(dimen)_2(dppm)_2^{3+}$. Hence, while the second $1e^-$ oxidation couple ($E^{\circ\prime}_{4+/3+}$) is +0.526 V more positive than the first ($E^{\circ\prime}_{3+/2+}$) for $Rh_2(dimen)_2(dppm)_2^{2+}$, it lies at approximately the same potential as $E^{\circ\prime}_{3+/2+}$ for $Rh_2(dimen)_3(dppm)^{2+}$ and is negative of $E^{\circ\prime}_{3+/2+}$ by more than 0.2 V for $Rh_2(dimen)_4^{2+}$.

Table I summarizes the temperature dependence of K_{disp}', as determined by variable-temperature electrochemical[23] and UV-vis-IR spectroelectrochemical techniques. Van't Hoff plots of these data yield respective values for $\Delta H_{disp}'$ and $\Delta S_{disp}'$ of +14000 cal/mol and +6.6 eu for $Rh_2(dimen)_2(dppm)_2^{3+}$; +1110 cal/mol and +3.8 eu for $Rh_2(dimen)_3(dppm)^{3+}$; and +1930 cal/mol and +23 eu for $Rh_2(dimen)_4^{3+}$. A comparison of the magnitudes of $\Delta H_{disp}'$ and $-T\Delta S_{disp}'$ for each of the three compounds indicates that both enthalpic and entropic factors make significant contributions to the value of K_{disp}'. Moreover, replacing two dimen ligands by two dppm ligands renders the disproportionation reaction enthalpically less favorable by 12 kcal/mol and entropically less favorable by nearly 5 kcal/mol at 25 °C.

Clearly, subtle changes in molecular structure play a key role in directing a given molecule toward multielectron-transfer pathways. At this time, we are investigating the large enthalpy and entropy changes that occur with the sequential replacement of dimen ligands by dppm. These changes must be significant, as K_{disp}' at room temperature encompasses a range of greater than 10^{12}. While in principle these changes can be manifest in any of the d^8-d^8, d^7-d^8, or d^7-d^7 electronic states, our data suggest they result primarily from differences in the thermodynamic stabilities of the various perchlorate bound $2e^-$ oxidized species. The direction of change in both $\Delta H_{disp}'$ and $\Delta S_{disp}'$ suggests that the pendant phenyl rings of the dppm ligands in the phosphine-substituted complexes interfere with the energetics of the arrangement and subsequent binding of perchlorate ligands to the Rh_2^{4+} cores by partially bloacking the axial sites.

Acknowledgment. We wish to thank Dr. John Bullock for several helpful discussions, Professor J. E. Ellis for the use of his FTIR spectrometer, and Johnson-Matthey, Inc., for a generous loan of rhodium trichloride.

(19) (a) Miskowski, V. M.; Smith, T. P.; Loehr, T. M.; Gray, H. B. *J. Am. Chem. Soc.* **1985**, *107*, 7925. (b) Shin, Y.; Miskowski, V. M.; Nocera, D. G. *Inorg. Chem.* **1990**, *29*, 2308.

(20) For experimental details regarding the spectroelectrochemical experiments, see: Bullock, J. P.; Mann, K. R. *Inorg. Chem.* **1989**, *28*, 4006.

(21) Miskowski, V. M.; Mann, K. R.; Gray, H. B.; Milder, S. J.; Hammond, G. S.; Ryason, P. R. *J. Am. Chem. Soc.* **1979**, *101*, 4383.

(22) $Rh_2(dimen)_3(dppm)^{3+}$ exhibits an EPR spectrum very similar to that of $Rh_2(dimen)_2(dppm)_2^{3+}$,[11a] with two signals centered at g = 2.27 and g = 1.99. We have not obtained the EPR spectrum of $Rh_2(dimen)_4^{3+}$.

(23) Values for $E^{\circ\prime}_{3+/2+}$ and $E^{\circ\prime}_{4+/3+}$ were determined for $Rh_2(dimen)_2(dppm)_2^{2+}$ by Osteryoung square-wave voltammetry.

(24) To whom correspondence should be addressed.

Department of Chemistry
University of Minnesota
Minneapolis, Minnesota 55455

Michael G. Hill
Kent R. Mann*[,24]

Received October 19, 1990

$[Na_9Fe_{20}Se_{38}]^{9-}$: A High-Nuclearity Bicyclic Cluster Constructed by the Fusion of Fe_2Se_2 Rhombs

The syntheses of high-nuclearity metal-oxide, -chalcogenide, and -pnictide clusters in soluble molecular forms[1-6] and within

(1) Schmid, G. *Struct. Bonding (Berlin)* **1985**, *62*, 51.

(2) Kharas, K. C. C.; Dahl, L. F. *Adv. Chem. Phys.* **1988**, *70* (2), 1.

(3) (a) Fenske, D.; Ohmer, J.; Hachgenei, J.; Merzweiler, K. *Angew. Chem., Int. Ed. Engl.* **1988**, *27*, 1277. (b) Fenske, D.; Hollnagel, A. *Angew. Chem., Int. Ed. Engl.* **1989**, *28*, 1390.

(4) (a) Lippard, S. J. *Angew. Chem., Int. Ed. Engl.* **1988**, *27*, 344. (b) Micklitz, W.; Lippard, S. J. *J. Am. Chem. Soc.* **1989**, *111*, 6856.

0020-1669/91/1330-1431$02.50/0

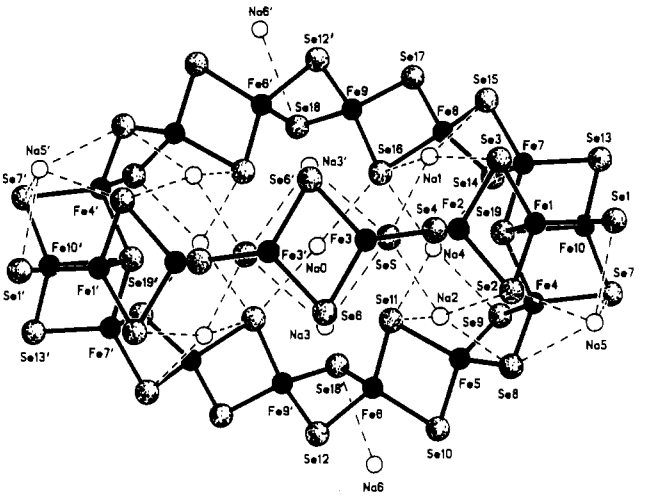

Figure 1. Structure of $[Na_9Fe_{20}Se_{38}]^{9-}$, including the atom-labeling scheme. Primed and unprimed atoms are related by an imposed C_2 axis that is passing through Na(0) and is perpendicular to the $Fe_2(3,3')Se_2$-(6,6') rhomb. Ranges and mean values of distances (Å) and angles (deg) are averaged under D_{3h} symmetry. Chains: Fe(1)–Fe(2) = 2.750–2.780, 2.76 (1); Fe(2)–Fe(3) = 2.790–2.843, 2.83 (3); Fe(3)–Fe(3′) = 2.760–2.780, 2.767 (9); Fe(1)–Se(2) = 2.323–2.349, 2.34 (1); Fe(1)–Se(3) = 2.336–2.383, 2.35 (2); Fe(2)–Se(2) = 2.361–2.377, 2.369 (7); Fe(2)–Se(3) = 2.370–2.381, 2.374 (5); Fe(2)–Se(4) = 2.334–2.358, 2.34 (1); Fe(2)–Se(5) = 2.397–2.436, 2.42 (2); Fe(3)–Se(4) = 2.329–2.365, 2.35 (1); Fe(3)–Se(5) = 2.376–2.422, 2.39 (2); Fe(3)–Se(6) = 2.349–2.404, 2.37 (2); Fe(3)–Se(6′) = 2.370–2.383, 2.375 (6); Se–Fe–Se = 103.6–117.6; Fe–Se–Fe = 71.0–75.1. Bridgehead rhombs: Fe(1)–Fe(10) = 2.864–2.886, 2.87 (1); Fe(1)–Se(1) = 2.294–2.333, 2.31 (2); Fe(1)–Se(19) = 2.516–2.541, 2.53 (1); Fe(10)–Se(19) = 2.438; Fe-(10)–Se(1) = 2.356–2.438, 2.39 (3); Se–Fe–Se = 106.2–108.4; Fe–Se–Fe = 70.2–76.1°. Na–Se = 2.87 (2)–3.28 (2). Esd's of individual distances and angles are 0.008–0.010 Å and 0.3°, respectively.

confining and stabilizing host structures such as zeolites[7,8] and inverse micelles[9] have recently been accomplished. These are two of the developments that demonstrate traversal of the gap between conventional molecular sizes and finite assemblies with dimensions of nanometers. Examples of large molecular chalcogenide clusters include $Ni_{20}Te_{18}(PEt_3)_{12}$[5] and $Ni_{34}Se_{22}(PPh_3)_{10}$,[3a] in which polynuclear structures are capped by phosphine terminal ligands. One unexplored class of compounds that potentially includes high-nuclearity structures are those chalcogenometalates $[M_xQ_y]^{2-}$ (Q = S, Se, Te) in which M is tetrahedral and Q is a bridging ligand ($\mu_{2,3,4}$) exclusively. A large number of structures can be assembled by edge- and apex-sharing of M_2Q_2 rhombs.[10] The first cluster of this type, *c*-$[Na_2Fe_{18}S_{30}]^{8-}$ (**1**), was recently prepared.[10] We report a second large cluster of unprecedented structure based on this principle.

A reaction mixture containing 20 mmol of $FeCl_3$ and 60 mmol of Na[PhNC(O)Me][10] in 60 mL of ethanol was treated over a period of 5 h with a solution prepared from 40 mmol of Li_2Se[11] in 90 mL of ethanol,[12] resulting in a dark brownish green color.

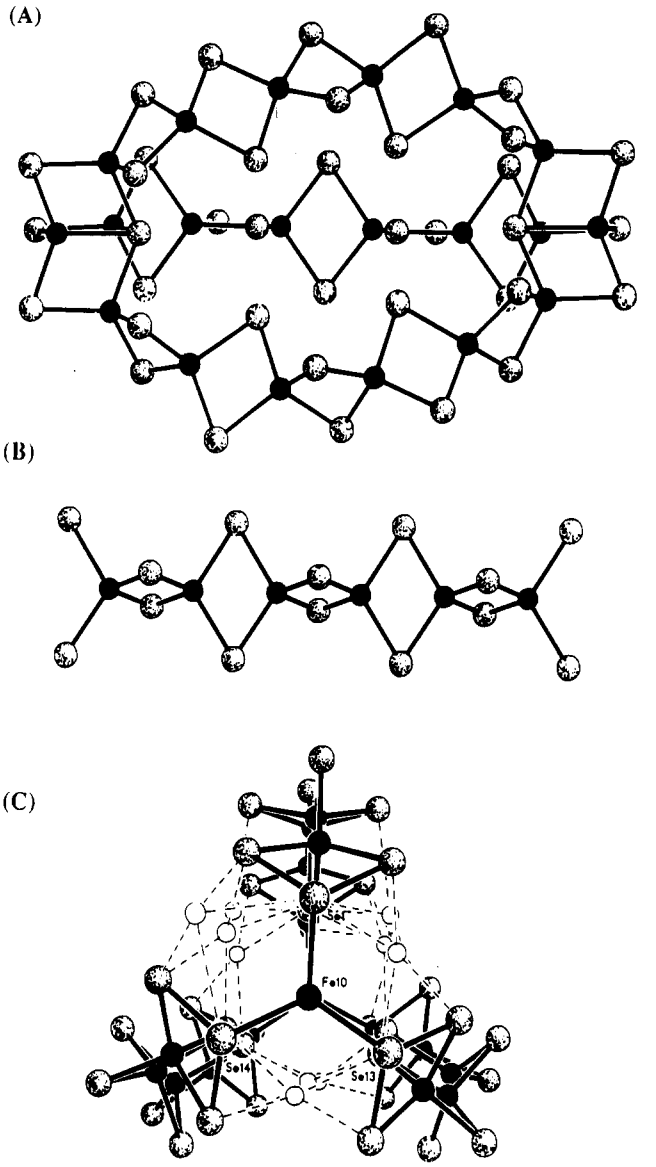

Figure 2. (A) Structure of cluster **2**, excluding sodium ions ($[Fe_{20}Se_{38}]^{18-}$). (B) Illustration of the Fe_6Se_{12} chain in linear form, with two additional Se atoms of each terminal Fe atom that are part of the bridgehead rhombs. (C) Depiction of the pseudo-C_3 axis of $[Na_9Fe_{20}Se_{38}]^{9-}$ along the Fe(10)–Fe(10′) vector.

The spectrum of the reaction mixture at this point (λ_{max} = 353, 446, 558, 673 nm) is a red-shifted version of the four-band spectrum of $[FeS_2]_n^{n-}$,[10] and accordingly is assigned to a chromophore that is mainly the chain or ring polymer $[FeSe_2]_n^{n-}$. The mixture was stirred for 12 h and filtered, and 30 mmol of Bu_4NBr in 15 mL of ethanol was added. Collection of the solid, which separated after 5–10 days, and recovery of additional material from the filtrate[12] afforded 4.4 g (70%, based on Fe) of a readily desolvated, black crystalline solid. The apparent formula from X-ray structural analysis is $(Bu_4N)_{4.5}Na_{13.5}Fe_{20}Se_{38}$·2PhNHCOMe·15EtOH.[12] When partially desolvated (room

(5) Brennan, J. G.; Siegrist, T.; Stuczynski, S. M.; Steigerwald, M. L. *J. Am. Chem. Soc.* **1989**, *111*, 9240.
(6) DiSalvo, F. J. *Science* **1990**, *247*, 649.
(7) (a) Herron, N.; Wang, Y.; Eddy, M. M.; Stucky, G. D.; Cox, D.; Moller, K.; Bein, T. *J. Am. Chem. Soc.* **1989**, *111*, 4141. See also: (b) Herron, N.; Wang, Y.; Eckert, H. *J. Am. Chem. Soc.* **1990**, *112*, 1322.
(8) Stucky, G. D.; MacDougall, J. E. *Science* **1990**, *247*, 669.
(9) (a) Steigerwald, M. L.; Alivasatos, A. P.; Gibson, J. M.; Harris, T. D.; Kortan, R.; Muller, A. J.; Thayer, A. M.; Duncan, T. M.; Douglass, D. C.; Brus, L. E. *J. Am. Chem. Soc.* **1988**, *110*, 3046. (b) Kortan, A. R.; Hull, R.; Opila, R. L.; Bawendi, M. G.; Steigerwald, M. G.; Carroll, P. J.; Brus, L. E. *J. Am. Chem. Soc.* **1990**, *112*, 1327 and references therein.
(10) You, J.-F.; Snyder, B. S.; Papaefthymiou, G. C.; Holm, R. H. *J. Am. Chem. Soc.* **1990**, *112*, 1067.
(11) Gladysz, J. A.; Hornby, J. L.; Garbe, J. E. *J. Org. Chem.* **1978**, *43*, 1204.

(12) Experimental data: All operations, manipulations, and measurements were performed under anaerobic conditions. The second crop of product was obtained by layering of 200 mL of *i*-PrOH on the filtrate after 50% volume reduction. Diffraction data were collected at 170 K with Mo Kα radiation; an empirical absorption correction was applied. Crystal data: a = 34.55 (1) Å, b = 26.169 (5) Å, c = 24.244(8) Å, Z = 4, space group *Pbcn*, 6238 unique data ($I \geq 3\sigma(I)$, $3° \leq 2\theta \leq 50°$). All Fe and Se atoms were located by direct methods and other non-hydrogen atoms by Fourier techniques. The nonstoichiometric formula arises from half of an interstitial EtOH molecule and a model based on mixed occupancy of Bu_4N^+ and $[Na(EtOH)_4]^+$ at one site. Refinement with Fe and Se atoms anisotropic and other atoms isotropic converged at R (R_w) = 9.9 (9.5)%.

temperature, 10 h, in vacuo), the apparent formula from analytical data is the 12EtOH solvate.[13] The compound forms brown-black solutions with λ_{max} = 361, 447, 562, 676 nm (acetonitrile).

The structure of the discrete $[Na_9Fe_{20}Se_{38}]^{9-}$ (**2**) cluster is depicted in Figure 1. Like **1**, the cluster contains *no* terminal ligands and thus is necessary cyclic, but unlike monocyclic **1**, it is a *bicyclic* cluster of ellipsoidal shape. An imposed C_2 axis lies perpendicular to the plane of the rhomb $Fe_2(3,3')Se_2(6,6')$. As shown in Figure 2AB, the structure consists of three $Fe_6(\mu_2\text{-}Se)_{10}$ chains, Fe(1)–Fe(1′), Fe(4)-Fe(7′), and Fe(7)-Fe(4′). Terminal atoms Fe(1,4,7) are each included in a bridgehead rhomb by μ_2-Se(1,7,13) bridges, the three rhombs being fused along the common edge Fe(10)-Se(19) to form the previously unknown tetranuclear fragment $[Fe_4(1,4,7,10)\text{-}\mu_2\text{-}Se_3(1,7,13)\text{-}\mu_4\text{-}Se(19)]$. A symmetry-related unit completes the structure on the opposite end. All Fe atoms in the structure are found in tetrahedral $FeSe_4$ units.

Cluster **2** approaches D_{3h} symmetry (Figure 2C), this being broken mainly by small twists in the Fe_6Se_{10} chains and by the positions of atoms Na(5,5′,6,6′) exterior to the cluster. The dihedral angles between bridgehead rhombs (119.5, 120.0, 120.5°) further emphasize the trigonal symmetry of the cluster. Because of the large number of independent parameters,[14] the metric values given in Figure 1 are organized under effective D_{3h} symmetry. These values are unexceptional when compared with related Fe–Se clusters with terminal ligands.[15,16] The alternating mean Fe–Fe distances in the chains (2.76, 2.83, 2.77 Å) are somewhat unusual and are absent in linear $[Fe_3Se_4(SPh)_4]^{3-}$ (Fe–Fe = 2.781 (1) Å).[16]

Within the cluster cavity are nine sodium ions (Na(0), Na(1–4), Na(1′–4′)), encapsulated in the manner of a cryptand and also coordinated to ethanol solvate molecules. These ions, which interact with Se atoms at 2.87–3.28 Å, are doubtless included to diminish the charge of the $[Fe_{20}Se_{38}]^{18-}$ core, especially when assembled in a nonaqueous solvent. Atom pairs Na(1,3′; 2,3; 0,4) and those symmetry-related are each bridged by one ethanol molecule. Exterior atoms Na(5,5′) are additionally coordinated by acetanilide while Na(6,6′) atoms are each bridged by two ethanol molecules to sodium ions exterior to another cluster, forming an infinite network. These interactions are easily disrupted for the compound is readily soluble in polar aprotic solvents.

This work provides a second demonstration that high-nuclearity chalcogenoferrates of unique structures are attainable by cluster assembly reactions. The cluster dimensions of **2**, 11.2 (2 × (centroid–Se(6)) × 17.4 Å (Se(1)-Se(1′)) show that it, like **1**, is in the nanometer size range. The structure is built by a combination of Fe_2Se_2 rhomb vertex sharing (chains) and edge fusion (bridgeheads). It is the first example of a bicyclic cluster. The Fe_6Se_{10} chains are presumably fragments of the initial $[FeSe_2]_n^{n-}$ polymer. Indeed, the absorption spectrum of **2** exhibits a four-band pattern closely analogous to that of the polymer. The cluster is mixed valence (18 Fe^{III} and 2 Fe^{II}) and has an $S = 0$ ground state. Its Mössbauer spectrum at 4.2 K can be fit with two quadrupole doublets[17] whose mean isomer shift (0.27 mm/s) is consistent with dominant Fe^{III} character. The formation of **1** and **2** implies that other large chalcogenoferrates may be assembled under different reaction conditions. Further, the structure of **2** suggests that its fragments, such as $Na_2Fe_2Se_4$, Fe_4Se_4, and Fe_6Se_{10}, may be available by cluster-cleavage reactions. Thus far, the core units Fe_2Se_2, Fe_3Se_4, Fe_4Se_4, Fe_6Se_6, and Fe_6Se_9 are known in clusters with terminal ligands.[15,16,18] The electronic and reactivity properties of cluster **2** will be the subject of a future report.

Acknowledgment. This research was supported by NIH Grant 28856. X-ray diffraction equipment was obtained by NIH Grant 1 S10 RR 02247. We thank Dr. G. C. Papaefthymiou for use of a Mössbauer spectrometer.

Supplementary Material Available: Table of atomic positional and isotropic thermal parameters for $(Bu_4N)_{4.5}Na_{13.5}Fe_{20}Se_{38}\cdot 2PhNHCOMe\cdot 15EtOH$ (3 pages). Ordering information is given on any current masthead page.

(13) Elemental analysis (C, H, Fe, N, Na, Se) are in excellent agreement with the formula; in addition, the atom ratio Se:Fe = 1.86 by EDS (calcd, 1.90).

(14) Under the actual C_2 symmetry, the independent dimensions of bonded atoms are 11 Fe–Fe and 40 Fe–Se distances and 60 Se–Fe–Se and 24 Fe–Se–Fe angles.

(15) (a) Bobrik, M. A.; Laskowski, E. J.; Johnson, R. W.; Gillum, W. O.; Berg, J. M.; Hodgson, K. O.; Holm, R. H. *Inorg. Chem.* **1978**, *17*, 1402. (b) Strasdeit, H.; Krebs, B.; Henkel, G. *Inorg. Chim. Acta* **1984**, *89*, L11. (c) Rutchik, S.; Kim, S.; Walters, M. A. *Inorg. Chem.* **1988**, *27*, 1515. (d) Carney, M. J.; Papaefthymiou, G. C.; Whitener, M. A.; Spartalian, K.; Frankel, R. B.; Holm, R. H. *Inorg. Chem.* **1988**, *27*, 346.

(16) (a) Ciurli, S.; Yu, S.-B.; Holm, R. H.; Srivastava, K. K. P.; Münck, E. *J. Am. Chem. Soc.* **1990**, *112*, 8169. (b) Yu, S.-B.; Holm, R. H. Submitted for publication.

(17) Current analysis gives these parameters (mm/s): δ_1 = 0.25, ΔE_{Q1} = 0.58 (68%); δ_2 = 0.30, ΔE_{Q2} = 1.10 (32%). Isomer shifts are relative to Fe metal at 4.2 K.

(18) (a) Strasdeit, H.; Krebs, B.; Henkel, G. *Z. Naturforsch.* **1987**, *42B*, 565. (b) Snyder, B. S.; Holm, R. H. *Inorg. Chem.* **1988**, *27*, 2339.

Department of Chemistry
Harvard University
Cambridge, Massachusetts 02138

Jing-Feng You
R. H. Holm*

Received October 16, 1990